Talanta 129 (2014) 328–335

Contents lists available at ScienceDirect

Talanta

journal homepage: www.elsevier.com/locate/talanta

Amplified electrochemical detection of protein kinase activity based on gold nanoparticles/multi-walled carbon nanotubes nanohybrids

Jinquan Liu [a,b], Xiaoxiao He [a,b,c,*], Kemin Wang [a,b,c,*], Yonghong Wang [a,b], Genping Yan [a,b], Yinfei Mao [a,c]

[a] State Key Laboratory of Chemo/Biosensing and Chemometrics, Key Laboratory for Bio-Nanotechnology and Molecule Engineering of Hunan Province, Hunan University, Changsha 410082, PR China
[b] College of Chemistry and Chemical Engineering, Hunan University, Changsha 410082, PR China
[c] College of Biology, Hunan University, Changsha 410082, PR China

ARTICLE INFO

Article history:
Received 27 February 2014
Received in revised form
5 May 2014
Accepted 7 May 2014
Available online 6 June 2014

Keywords:
Protein kinase A (PKA)
Electrochemical
AuNPs/MWNTs nanohybrids
Peroxidase-like activity
Inhibitor

ABSTRACT

A sensitive and simple electrochemical strategy has been developed for assay of protein kinase A (PKA) activity and inhibition using gold nanoparticles/multi-walled carbon nanotubes (AuNPs/MWNTs) nanohybrids. Key features of this assay included intrinsic peroxidase-like activity of positively-charged gold nanoparticles (+AuNPs) and signal transduction and amplification of multi-walled carbon nanotubes (MWNTs). In this assay, an N-terminally cysteine-containing peptide was self-assembled onto the gold electrode via Au–S bonding and used as substrate for PKA, and adenosine-5′-(γ-thio)-triphosphate was used as co-substrate. Upon thiophosphorylation in the presence of PKA, the AuNPs/MWNTs nanohybrids would be fixed onto the peptides via Au–S bond. The conjugated AuNPs/MWNTs nanohybrids could catalyze the 3, 3′, 5, 5′-Tetramethylbenzidine (TMB) oxidation by H_2O_2 to form TMB oxidation product, which was reduced at the electrode surface to generate an electrochemical current. It was eT on state. The current signal intensity is proportional to the activity of PKA. Here, the presence of MWNTs not only increased the surface area for accumulation of +AuNPs but also could promote electron-transfer reaction. It was found that the electrochemical strategy can be employed to assay PKA activity with a low detection limit of 0.09 U/mL. The linear range of the assay for PKA enzymatic unit/ml was 0.1–1 U/mL. Furthermore, the interferences experiments of T4 polynucleotide kinase (T4 PNK) and Casein kinase II (CK2), and inhibition of PKA, have also been studied by using this strategy. The developed method would provide a diversified platform for kinase activity and inhibition monitoring.

1. Introduction

Protein kinases, as one type of kinase enzymes, are committed to catalyze the transfer of the γ-phosphate group from ATP to the hydroxyl groups of serine, threonine, or tyrosine in protein substrate. By adding phosphate groups to substrate proteins, the protein kinases direct the activity, localization and overall function of many proteins, and serve to orchestrate the activity of almost all cellular processes [1,2]. It has been reported that the abnormal activity and expression of protein kinases are related to various diseases such as cancer [3], diabetes [4] and Alzheimer's disease [5]. Hence, the accurate monitoring and analyzing of the protein kinase activity and their potential inhibitors are not only essential for providing insights regarding the fundamental mechanisms in basic biology but also necessary to the clinical diagnostics.

Up to now, many techniques for protein kinase activity detection have been developed, including ^{32}P radioisotope [6], fluorescently-based assay [7–10], mass spectroscopy (MS) [11], surface plasmon resonance (SPR) [12] and quartz crystal microbalance (QCM) [13]. These methods are effective but they are limited by the drawback of high risk of radioactive contamination, time-consuming, expensive and sophisticated operating procedures. Recently, electrochemical methods attracted substantial research interest in protein kinase detection owing to the advantages of simplicity, rapid response, sensitivity, and cost-effective [14–20]. Especially some novel and high sensitive electrochemical detection strategies for protein kinases assay were proposed by sharing unique physicochemical properties of the recently developed nanomaterials [21–23]. Up to now, the widely used nanomaterials for constructing electrochemical protein kinases detection methods were mainly focused on two types of nanomaterials. One is TiO_2 nanoparticles or TiO_2 based nanocomposites [24,25]. Based on the capability to selectively bind phosphate

* Corresponding authors at: State Key Laboratory of Chemo/Biosensing and Chemometrics, Key Laboratory for Bio-Nanotechnology and Molecule Engineering of Hunan Province, Hunan University, Changsha 410082, PR China. Tel./fax: +86 731 88821566.
E-mail addresses: xiaoxiaohe@hnu.edu.cn (X. He), kmwang@hnu.edu.cn (K. Wang).

http://dx.doi.org/10.1016/j.talanta.2014.05.043
0039-9140/

functional groups, TiO_2 nanoparticles or TiO_2 based nanocomposites could be easily conjugated to phosphorylated peptides modified electrodes and were used for protein kinases detection with simplicity and high sensitivity. The other is gold nanoparticles (AuNPs). The AuNPs have unique properties, such as size- and shape-dependent optical and electronic features, a high surface area to volume ratio, and easy modification with ligands [26,27]. By taking advantages of the high surface area and fast electron transfer rate of AuNPs, some AuNPs-based electrochemical biosensors for protein kinase activity detection have been developed [28,29]. For example, Wang et al. used amplification efficiency of AuNPs to develop an enzyme-linked electrocatalysis strategy for kinase activity and inhibition analysis [30]. Xu et al. reported an electrochemiluminescence (ECL) biosensor for kinase activity and inhibition analysis by using the fast electron transfer rate of AuNPs [31]. Apart from the above mentioned unique properties, AuNPs have also been demonstrated to catalyze oxidation owning to the surface properties of AuNPs. The surface properties were influenced by the groups which modified on the surface of AuNPs. The surface properties of AuNPs could influence the absorption of H_2O_2 and the particle-mediated electron transfer processes, and then affect the catalytic ability of +AuNPs [32,33]. For instance, the positively charged AuNPs (+AuNPs), capped with cysteamine, possess intrinsic peroxidase-like activity, which can catalyze oxidation of the peroxidase substrate 3, 3′, 5, 5′-Tetramethylbenzidine (TMB) by H_2O_2 to form TMB oxidation product. Based on this principle, the +AuNPs-based colorimetric sensors have been developed and used for detecting H_2O_2 and glucose [34,35]. However, the catalysis of +AuNPs has not been reported for protein kinases activity detection, especially in electrochemical assay. In addition, carbon nanotubes (CNTs), composed of hollow graphitic cylinders, represent a kind of prospective nanomaterials. Due to the high electronic conductivity, unique electronic structure, and large specific surface area, CNTs are promising as an immobilization substance for developing electrochemical biosensors [36]. Thus, the ability to integrate the peroxidase-like activity of +AuNPs and fast electron transfer rate of CNTs for developing sensitive protein kinase activity and inhibition assay is very encouraging.

Herein, we developed a sensitive and simple electrochemical strategy for assay of protein kinase A (PKA) activity and inhibition based on gold nanoparticles/multi-walled carbon nanotubes (AuNPs/MWNTs) nanohybrids. This strategy takes advantages of intrinsic peroxidase-like activity of +AuNPs and signal transduction and amplification of MWNTs. As shown in Scheme 1, in the detection system, when the substrate peptide self-assembled on the electrode was phosphorylated by PKA using adenosine 5′-[γ-thio] triphosphate tetralithium salt (ATP-S) as the co-substrate, the AuNPs/MWNTs nanohybrids were then conjugated onto the peptide via Au–S bond. The conjugated AuNPs/MWNTs nanohybrids could catalyze TMB by H_2O_2 to form TMB oxidation product, which was reduced at the electrode surface to generate an electrochemical current signals [37,38]. The generated peak currents were related to the enzymatic unit/ml of the PKA, providing a sensing platform for monitoring PKA activity and inhibition. To the best of our knowledge, it is the first time that the peroxidase-like activity of +AuNPs is used for electrochemical analysis of protein kinase activity and inhibition. This strategy provides a simple, sensitive, selective, and universal platform for protein kinase activity assay and inhibitor screening.

2. Experimental

2.1. Chemicals and materials

The N-terminally cysteine-containing substrate peptide of PKA (CLRRASIG) was synthesized and purified by Sangon Biological Engineering Technology & Services Co., Ltd. (Shanghai, China). Protein kinase A (PKA, recombinant c-AMP dependent protein kinase A catalytic subunit alpha; batch number: 228-11306; enzyme units: 15,000 units) was obtained from Ray Biotech, Inc. Casein kinase II (CK2, Isolated from a strain of *Escherichia coli* expressing both α and β CK2 subunits derived from a human glioblastoma cDNA library; batch number: P6010S; enzyme units: 10,000 units) and T4 polynucleotide kinase (T4 PNK, isolated from a strain of E. coli; batch number: M0201L; enzyme units: 500 units) were obtained from New England Biolabs, Inc. Adenosine 5′-[γ-thio] triphosphate tetralithium salt (ATP-S), adenosine 3′, 5′-cyclic monophosphate sodium salt monohydrate (cAMP), cysteamine, 3,3′,5,5′-Tetramethylbenzidine(TMB), 1-Ethyl-3-(3-dimethyl aminopropyl) carbodiimide hydrochloride (EDC), N-hydroxysuccinimide (NHS) and 6-Mercapto-1-hexanol (MCH) were purchased from Sigma-Aldrich. Multi-wall carbon nanotubes (MWNTs, purity >90%, diameter <10 nm, length 5–15 μm) were purchased from Nanoport. Co. Ltd. (Shenzhen, China). Hydrogen tetrachloroaurate trihydrate ($HAuCl_4 \cdot 3H_2O$) was purchased from Beijing Chemicals. Sodium borohydride ($NaBH_4$) and hydrogen peroxide (H_2O_2) were obtained from Sinopharm Chemical Reagent Co., Ltd. Tris (2-carboxyethyl) phosphine hydrochloride (TCEP) and ellagic acid were purchased from TCI Development Co., Ltd. (Shanghai, China). All other chemicals were obtained from Reagent & Glass Apparatus Corporation of Changsha and were of analytical grade used without further purification. The PKA storage buffer was 25 mM potassium phosphate (pH 6.5) containing 5 mM 2-mercaptoethanol, 5 mM EDTA, 150 mM NaCl, 50% glycerol. The PKA reaction buffer was 40 mM Tris–HCl containing 20 mM $MgCl_2$, pH 7.4. The washing buffer was 10 mM Tris–HCl containing 0.05% Tween-20, pH 7.4. Ultrapure water (Milli-Q 18.2 MΩ, Millipore System Inc.) was used for all the experiment.

2.2. Apparatus

The electrochemical measurements of electrochemical impedance spectroscopy (EIS) and square wave voltammograms (SWV) were performed on a CHI660A electrochemical workstation (Shanghai Chenhua Instrument Corporation, China). A conventional three-electrode system, consisting of a 2.0-mm diameter gold working electrode, a saturated calomel reference electrode (SCE), and a platinum wire counter electrode, was used in all electrochemical measurements. SWV experiments were obtained by scanning the potential from 0.1 V to 0.6 V with a step potential of 4 mV, pulse amplitude of 25 mV, and frequency of 15 Hz. EIS measurements were obtained within the frequency range from 0.01 Hz to 100 kHz; the amplitude of the applied sine wave potential was 5 mV. The electrolyte solution for EIS experiments was 10 mM PBS containing 5 mM $[Fe(CN)_6]^{3-/4-}$ and 0.3 M NaCl. In addition, the characteristics of the prepared AuNPs/MWNTs nanohybrids were detected by using transmission electron microscopy (TEM, JEM-3010, JEOL), scanning electron microscopy (SEM, S-4800, Hitachi), zetasizer 3000HS (Malvern, UK), energy dispersive X-ray (DU-5000, Siemens) and DU-800 Spectrophotometer (Beckman, America).

2.3. Electrochemical detection principle

The schematic diagram of this sensitive electrochemical strategy for the amplified detection of protein kinase activity based on AuNPs/MWNTs nanohybrids is illustrated in Scheme 1. The PKA specific substrate peptide was self-assembled onto the surface of the gold electrodes through its cysteine end and formed a dense assemble layer. To prevent the nonspecific adsorption, MCH was incubated on the blank binding sites. After the substrate peptide was phosphorylated by PKA in the presence of ATP-S, the thiophosphate group was transferred from the ATP-S to the substrate

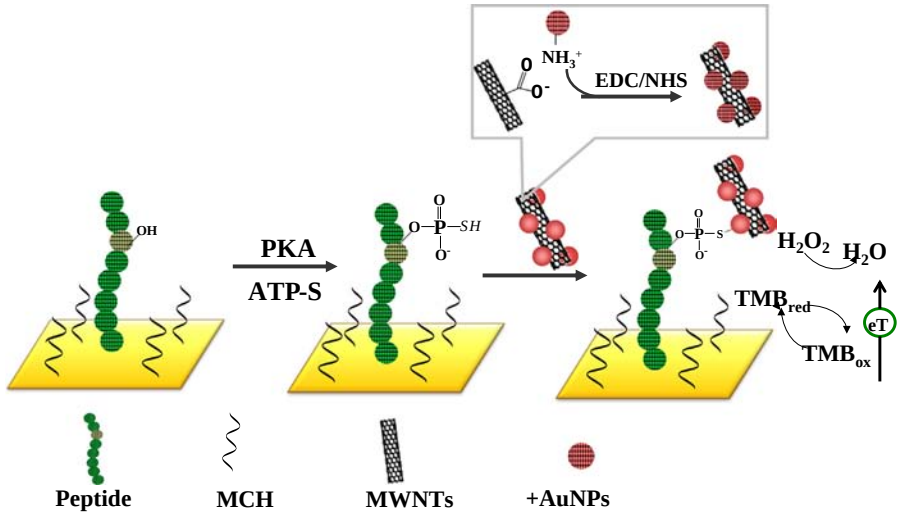

Scheme 1. The schematic illustration of the electrochemical principle for the assay of PKA activity using AuNPs/MWNTs nanohybrids.

peptide. Then the AuNPs/MWNTs nanohybrids could be conjugated to the thiol-functionalized substrate peptide through the chemical interaction between chemical functional group and AuNPs, resulting in the immobilization of AuNPs/MWNTs nanohybrids onto the electrodes. Subsequently, the peroxidase-like activity of AuNPs/MWNTs nanohybrids could catalyze the oxidation of TMB in the presence of H_2O_2 and amplified the electrochemical current. It was eT on state. The generated current signal could quantitatively reflect the activity of PKA. As a comparison, little AuNPs/MWNTs nanohybrids were absorbed on the unphosphorylated substrate peptide modified electrode. Thus, a weak electrochemical current signal was achieved in the absence of PKA.

2.4. Synthesis of the +AuNPs

Here, the +AuNPs were synthesized by $NaBH_4$ reduction of hydrogen tetrachloroaurate (III) ($HAuCl_4 \cdot 3H_2O$) in the presence of cysteamine according to the literature with little modification [39]. Briefly, a cysteamine solution (21 μL, 1 M) was added to 10 mL of 1.42 mM $HAuCl_4$ solution. After stirring for 20 min at room temperature, 10 μL of 10 mM $NaBH_4$ solution was added, and the mixture was vigorously stirred for 15 min at room temperature in the dark. Then, the mixture was further stirred for 25 min. When the solution changed from yellow to wine red, it indicated that the +AuNPs were formed, and the resulting solution was stored in the refrigerator (4 °C) and ready for use.

2.5. Preparation of AuNPs/MWNTs nanohybrids

MWNTs were functionalized following literature [40]. Briefly, MWNTs were sonicated for 20 h in 3:1 H_2SO_4/HNO_3 (v/v) mixture solution at a frequency of 40 KHz, and then the resulting dispersion was separated and washed with water by centrifugation (10,000 rpm) until the pH of the MWNTs solution was 7. The resulting functionalized MWNTs were dried under vacuum overnight. Thus, the MWNTs were functionalized with carboxylic acid groups and became water-soluble during the oxidation process.

The +AuNPs attachment onto MWNTs was carried out through an EDC/NHS amidization protocol. Firstly, 1 mL 1 mg/mL functionalized MWNTs were sonicated at a frequency of 40 KHz for 1 h to obtain a homogeneous dispersion, and then the dispersion was mixed with an EDC/NHS mixture (200 mM EDC and 50 mM NHS) and vortexed for 30 min to get activated MWNTs. Secondly, 6 mL +AuNPs solution was placed in a vial, followed by addition of 1 mL 1 mg/mL activated MWNTs solution and stirred overnight at room temperature. Ultimately, the AuNPs/MWNTs nanohybrids were synthesized. Then, the mixture was washed thoroughly with water and dried.

2.6. Substrate peptides immobilization on gold electrodes

Before immobilization of substrate peptides, the gold electrodes were firstly dipped in freshly prepared piranha solution (H_2SO_4:30% H_2O_2=3:1 v/v) for 10 min and cleaned by ultrapure water thoroughly. After that, the electrodes were polished with 0.3 and 0.05 μm alumina powder and sonicated sequentially in distilled water, ethanol and distilled water for 5 min each. Then, the electrodes were electrochemically cleaned in 0.5 M H_2SO_4 with potential scanning from −0.2 to 1.55 V until a reproducible cyclic voltammogram (CV) was obtained. After cleaning and dried with nitrogen, 20 μL of 250 mg/mL N-terminally cysteine-containing peptide solution (0.05 M PBS, containing 10 mM TCEP, pH 7.5) was dropped on the pre-cleaned gold electrodes' surface and incubated in darkness for 15 h at 4 °C. TCEP, here, was used to prevent substrate peptides from forming disulphide bonds. The resulting peptides modified electrodes were rinsed thoroughly with blank Tris–HCl buffer solution (10 mM, pH 7.4), followed by immersion in 1 mM MCH for 30 min to block the remaining bare region on the electrode. Finally, the peptide immobilization on electrodes was rinsed with blank buffer and ready for phosphorylation. The surface coverage of peptide on the gold electrode was determined using the quartz crystal microbalance method [28]. It was estimated to be 3.92×10^{-10} mol/cm^2, as described in the Supporting information.

2.7. PKA-catalyzed phosphorylation and its inhibition

The PKA-catalyzed phosphorylation reaction was performed by incubating the substrate peptides modified gold electrodes in 20 μL of kinase reaction buffer (40 mM Tris–HCl containing 60 μM ATP-S, 200 μM cAMP and 20 mM $MgCl_2$, pH 7.4) that contained a certain desired amount of PKA at 30 °C for 1 h. After that, the reaction was terminated by rinsing the electrode thoroughly with the blank buffer. The inhibition study was similar to the assay of PKA. During this study, a desired concentration of ellagic acid dissolved in the PKA assay buffer was used to check the inhibition of ellagic acid to PKA.

2.8. Electrochemical detection of PKA activity

The thiol-functionalized substrate peptide modified electrodes were incubated in 20 μL 0.5 mg/ml AuNPs/MWNTs nanohybrids at room temperature for 30 min. The AuNPs/MWNTs nanohybrids were then adsorbed onto the phosphorylated electrode surface through the gold–sulfur bond. After that, the electrodes were rinsed using the blank buffer to avoid non-specific adsorption.

For the detection of PKA activity, the resulting electrode was characterized by SWV in an assay buffer (0.1 M PBS containing 0.3 M KCl, 0.5 mM TMB and 5 mM H_2O_2, pH 5.0). To avoid the interference from the reduction of oxygen, the assay buffer was purged with high purity nitrogen for 10 min before the measurements. To perform the AuNPs/MWNTs nanohybrids-based catalytic reaction, the resulting electrodes were firstly immersed in the assay buffer for 15 min, and then measured with electrochemical instruments.

3. Results and discussion

3.1. Characterization of AuNPs/MWNTs nanohybrids

The morphology and microstructure of AuNPs/MWNTs nanohybrids were verified with TEM and SEM, respectively. To both of the untreated +AuNPs and MWNTs, we only observed the dispersed AuNPs or MWNTs in the TEM images (Fig. S2A and B). After attaching the +AuNPs onto MWNTs through an EDC/NHS method, it can be obviously seen that the +AuNPs with an average size of 25 nm were deposited on the MWNTs surface and no dispersed AuNPs could be observed in the background region (Fig. 1A and B). Furthermore, the EDX analysis was employed to characterize the AuNPs/MWNTs nanohybrids (Fig. 1C). The EDX results revealed the existence of Au element in the nanohybrids whereas C and O elements came from the MWNTs which functionalized with carboxylic acid group. In addition, the additional copper signal is a result of electrons scattered by the sample striking the Cu grid. We also used the EDX analysis to characterize the +AuNPs and MWCNT. The results of the EDX analysis are shown in Fig. S3. As shown in Table S1, the atomic percent of Au was 1.54%. However, it was increased to 7.16% after the +AuNPs attached on MWNTs–COOH with EDC/NHS coupling. It indicated that there were many +AuNPs on the MWNTs. The zeta potentials of the +AuNPs, carboxylated MWNTs and AuNPs/MWNTs nanohybrids were measured in water by Zetasizer 3000HS (Fig. S4). The surface charges of +AuNPs (a), carboxylated MWNTs (b) and AuNPs/MWNTs nanohybrids (c) were about 36.1 mV, −42.0 mV and −24.5 mV, respectively. The changes of surface charges also indicate that the AuNPs could successfully bond to carboxylated MWNTs. To further confirm the AuNPs were effectively bonded to carboxylated MWNTs, a UV–vis adsorption spectrum (Fig. S5) of the +AuNPs, MWNTs and the AuNPs/MWNTs nanohybrids was respectively measured by the DU-800 Spectrophotometer. The corresponding results displayed that the +AuNPs (a) had a strong absorption bands at 526 nm, and the MWNTs (b) had an absorption bands at 243 nm. While the AuNPs/MWNTs nanohybrids (c) had two strong absorption bands at 243 and 528 nm.

3.2. Characterization of electrodes modification

The modification results were confirmed by SEM image. Fig. 2A shows the image of the bare gold substrate. It appeared as a

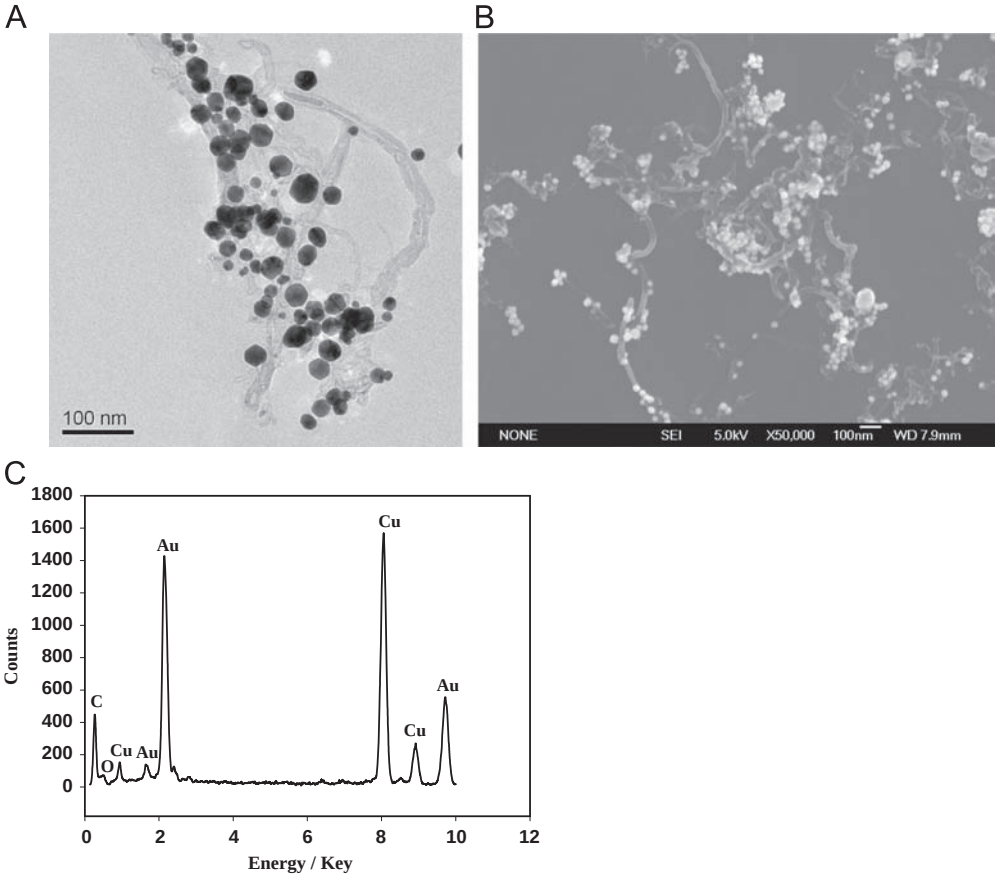

Fig. 1. Characterization of AuNPs/MWNTs nanohybrids. (A) TEM image of AuNPs/MWNTs nanohybrids. (B) SEM image of AuNPs/MWNTs nanohybrids. (C) EDX spectrum of AuNPs/MWNTs nanohybrids.

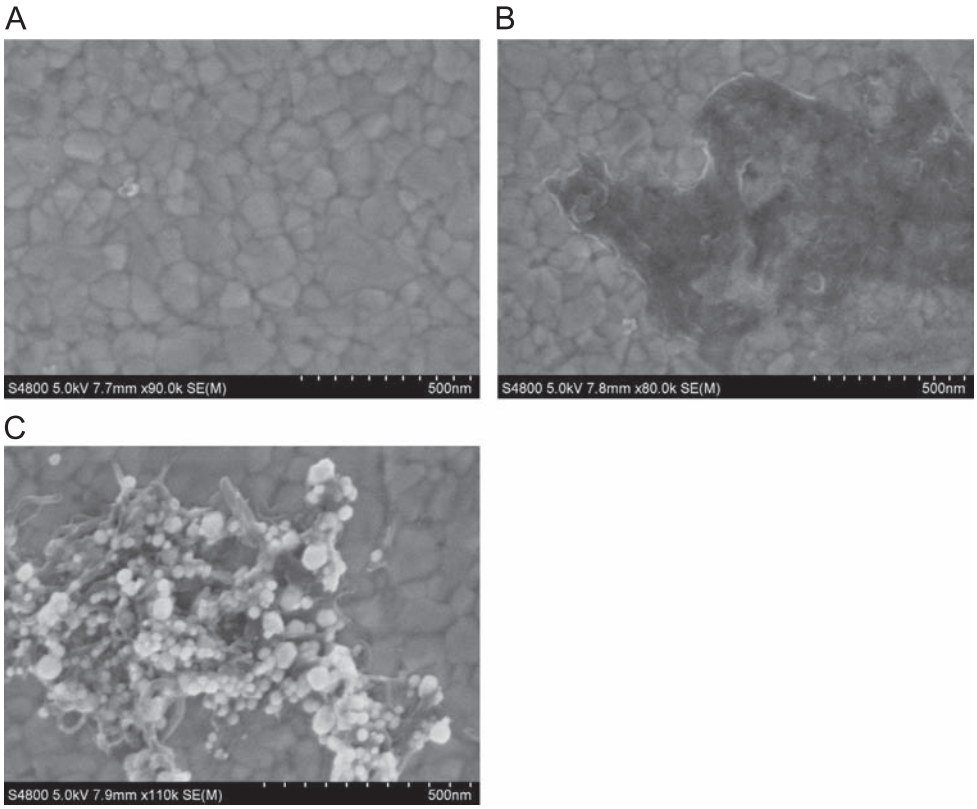

Fig. 2. SEM images of bare Au electrode (A), substrate peptide modified Au electrode blocked by MCH (B), and substrate peptide modified Au electrode after treating with AuNPs/MWNTs nanohybrids (C).

smooth and homogeneous surface. After the substrate peptide and MCH were modified on the gold substrate, we can see an area which was darker than surrounding (Fig. 2B). It was due to the poor conductivity of substrate peptide and MCH. The fact suggested that the substrate peptide and MCH were successfully assembled onto the gold substrate surface. As shown in Fig. 2B, it seems that the whole electrode was not covered by MCH and peptide which may contribute to cleaning and drying. Fig. 2C illustrates image of AuNPs/MWNTs nanohybrids immobilized on the gold substrate surface after the substrate peptide phosphorylation catalyzed by PKA in the presence of ATP-S. A large number of AuNPs/MWNTs nanohybrids appeared, which confirmed the assembly of AuNPs/WNTs nanohybrids on the modified electrode. In addition, some control experiments were also provided. As shown in Fig. S6A, lots of +AuNPs appeared on the gold substrate surface after the substrate peptide was phosphorylated by PKA. However, because of the nonspecific adsorption, a small number of AuNPs/WNTs nanohybrids appeared on the gold substrate surface which was modified with MCH alone (Fig. S6B). At the same time, there were also little +AuNPs (Fig. S6C) or AuNPs/WNTs nanohybrids (Fig. S6D) assembled on the gold substrate surface without the action of PKA.

The EIS measurement is an effective method for probing the interfacial properties of modified electrodes. Here, we used it to monitor the modification process of the electrodes. As Fig. 3A shows, attributing to fast electron-transfer process, the bare Au electrode revealed a very small semicircular domain and the resistances (Ret) value was 154.4 Ω (a). Because of the poor conductivity of substrate peptide and MCH, the electron-transfer resistance (Ret) increased to 4339 Ω (curve b) with the immobilization of the substrate peptide and MCH self-assembled onto the bare electrode via Au–S binding. After phosphorylation by PKA, the Ret further increased to 4910 Ω (curve c), which was due to the negatively charged phosphorylation sites blocked the electron transfer between the electrode surface and redox probes. After hybridization with AuNPs/MWNTs nanohybrids, the Ret decreased to 1080 Ω (curve d). The reason for this was that the AuNPs/MWNTs nanohybrids can promote electron-transfer processes. According to the EIS results, the modification process of the electrode was achieved successfully.

3.3. Feasibility investigation of the electrochemical assay

After characterizing the electrode modification, the feasibility of this designed strategy was investigated by using SWV measurements. The SWV responses were recorded after the substrate peptides were phosphorylated by PKA and linked with AuNPs/MWNTs nanohybrids via Au–S bonding. As shown in Fig. 3B, the thiol-functionalized substrate peptide modified electrode exhibited a weaker signal (curve a). However, when the AuNPs/MWNTs nanohybrids assembled onto the thiol-functionalized substrate peptide modified electrode, a strong electrochemical signal at 0.25 V was observed (curve b), which was associated with the oxidation of TMB catalyzed by AuNPs/MWNTs nanohybrids in the presence of H_2O_2. In addition, some control experiments were carried out by treating with +AuNPs (curve c) and AuNPs/MWNTs nanohybrids (curve d) without the action of PKA. The electrochemical signal on the substrate peptide modified electrode after treatment of +AuNPs and AuNPs/MWNTs nanohybrids was weak but showed a slight increase as compared with the curve a. These responses could arise from the nonspecific adsorption of nanoparticles. On the other hand, the SWV response was also increased after the thiol-functionalized substrate peptide modified electrode was treated with +AuNPs (curve e) owing to the peroxidase-like activity of +AuNPs. However, AuNPs/MWNTs nanohybrids had a higher electrochemical signal than that of +AuNPs. It demonstrated that the AuNPs/MWNTs nanohybrids could

potentially be used as an electrochemical signal amplifier. Thus, these results showed that the electrochemical assay for PKA activity could be carried out.

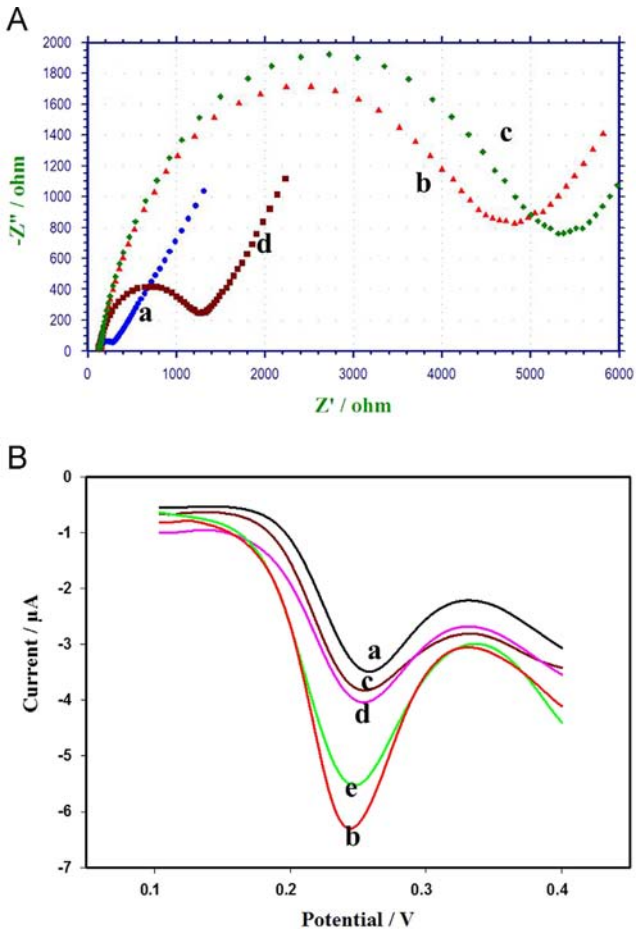

Fig. 3. (A) Nyquist plots obtained with bare Au eletrode (curve a), substrate peptide modified Au electrode blocked by MCH (curve b), substrate peptide/MCH modified Au electrode after phosphorylation by PKA (curve c) and substrate peptide modified Au electrode after phosphorylation by PKA and treat with AuNPs/MWNTs nanohybrids (curve d). (B) SWV response of substrate peptide modified electrode before (curve a) and after the assembly of AuNPs/MWNTs nanohybrids (curve b) and +AuNPs (curve e). Substrate peptide modified Au electrode without phosphorylation but treatment with +AuNPs (curve c) and AuNPs/MWNTs nanohybrids (curve d).

3.4. Optimization of experimental conditions

3.4.1. Optimization of ATP-S concentration

In order to optimize the experimental conditions, a series of experimental parameters were investigated in this work. The ATP-S offered the phosphate groups during the phosphorylation reaction. Therefore, the influence of the concentration of ATP-S was examined. As shown in Fig. S7A, the electrochemical signal intensity increased with the increase of the concentration of ATP-S concentration and reached a maximal value at the ATP-S concentration of 60 μM in the presence of 100 U/mL PKA. Thus, 60 μM ATP-S was sufficient to offer phosphate groups in this kinase reaction.

3.4.2. Optimization of phosphorylation time

The phosphorylation time is an important parameter for the kinase-catalyzed reaction. We monitored it by stopping the reaction at different time intervals and analyzing electrochemistry signals output correspondingly. As shown in Fig. S7B, the electrochemical signal intensity increased gradually as the phosphorylation time increased from 10 to 90 min with 60 μM ATP-S, and it reached the steady state over 60 min. Phosphorylation time higher than 60 min did not steeply increase in the current response. Therefore, the reaction of 60 min was chosen as the appropriate time in further experiments.

3.4.3. pH optimization of the AuNPs/MWNTs nanohybrids catalyzed hydrogen peroxide

Furthermore, like other nanomaterial-based peroxidase mimics [41], the peroxidase-like activities of AuNPs/MWNTs nanohybrids were also strongly dependent on pH. We here examined the influence of pH in the range 3.0–8.0 under the phosphorylation time; and concentrations of ATP-S were 60 min and 60 μM, respectively. From the results shown in Fig. S7C, the signal intensity gradually increased as the pH increased from 3.0 to 5.0, but it decreased at pH values higher than 5.0. Hence, this value was used in all subsequent experiments.

3.5. PKA activity detection

The protein kinase activity detection with different enzymatic unit/ml of PKA (from 0 to 100 U/mL) has been carried out under the optimal conditions. As shown in Fig. 4A, the amplified electrochemical signal increased linearly with PKA at lower enzymatic unit/ml and then slowed down at higher enzymatic unit/ml.

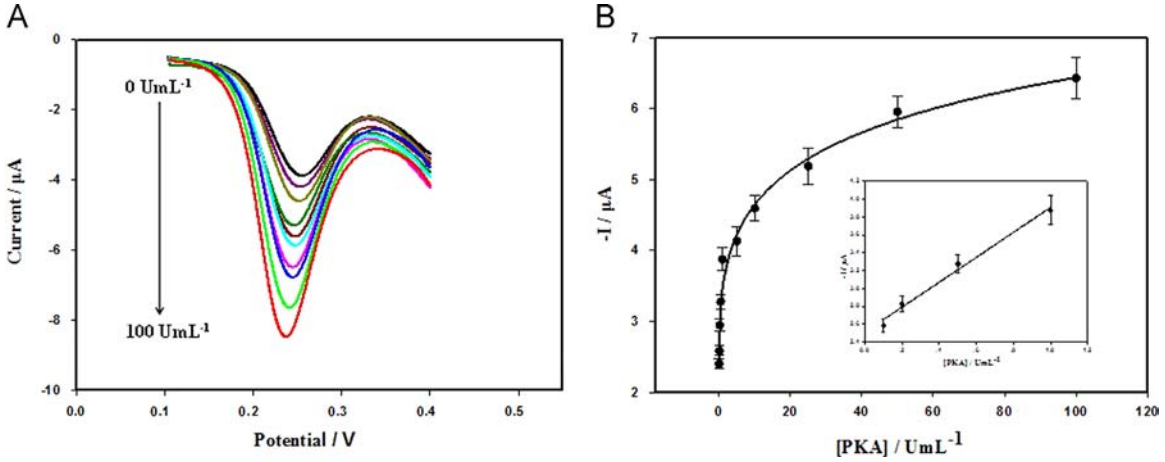

Fig. 4. (A) SWV response of AuNPs/MWNTs nanohybrids modified Au electrodes in N_2 saturated PBS (0.1 M, pH 5.0) containing 0.3 M KCl, 0.5 mM TMB and 5 mM H_2O_2 at different enzymatic unit/ml of PKA. The enzymatic unit/ml of PKA were 0, 0.1, 0.2, 0.5, 1, 5, 10, 25, 50, 100 U/mL. (B) Calibration curve of the PKA activity. Inset shows linear relationship between the current and the enzymatic unit/ml of the PKA from 0.1 U/mL to 1 U/mL.

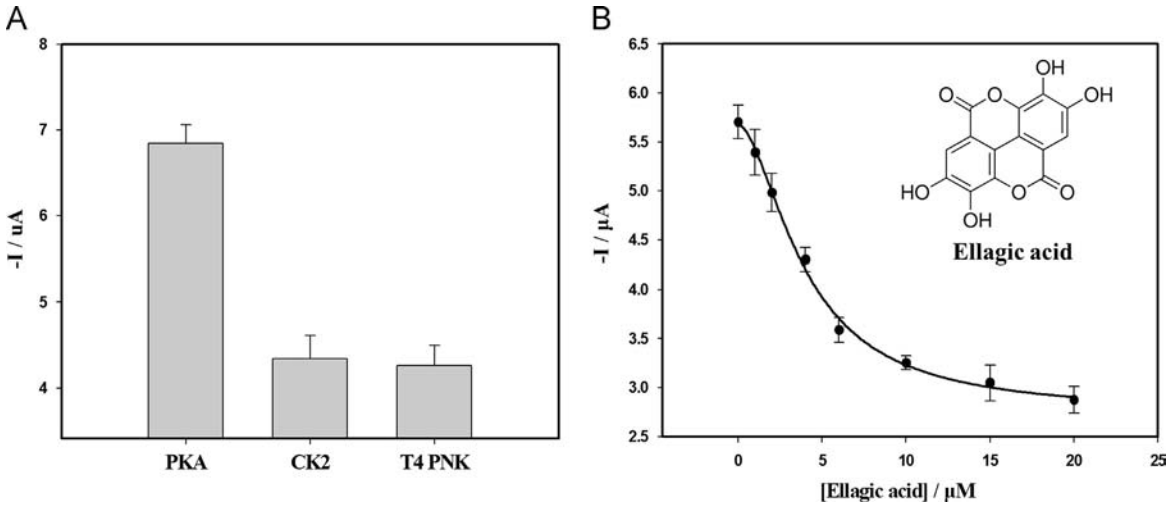

Fig. 5. (A) Selectivity of the electrochemical assay for PKA activity. The PKA, CK2 and T4 PNK were all tested at an enzymatic unit/ml of 100 U/mL. (B) Inhibition of the activity of PKA by ellagic acid in the presence of 100 U/mL PKA. The concentrations of ellagic acid were 0, 1, 2, 4, 6, 10, 15 and 20 μM.

Linear correlation showed in the calibration plot between the electrochemical signal and PKA enzymatic unit/ml in the range of 0.1–1 U/mL with a correlation coefficient of 0.9866 (inset in Fig. 4B). Analyzing the results with linear regression method, an equation of linear regression $-I=1.461c+2.466$ was obtained, where I referred to the electrochemical signal and c referred to the enzymatic unit/ml of PKA. The detection limit of PKA was 0.09 U/mL ($S/N=3$), which was lower than that of the previous reported assays [24,28]. This demonstrated that the proposed electrochemical assay can be employed for highly sensitive PKA activity detection.

In addition, we chose T4 PNK (catalyze the transfer of the γ-phosphate from ATP to the 5′-terminus of nucleic acids and oligonucleotides) and CK2 (catalyze the phosphorylation of RRADDSDDDDD) as interference factors. As shown in Fig. 5A, the electrochemical signal of the substrate peptide (CLRRASIG) modified gold electrode incubated with T4 PNK (100 U/mL) and CK2 (100 U/mL) was much smaller than the signal of the PKA (100 U/mL) in the presence of AuNPs/MWNTs nanohybrids. The results demonstrated that the interference factors of T4 PNK and CK2 could not catalyze phosphorylation of the CLRRASIG sequence, which indicated that the electrochemical assay has good specificity.

The reproducibility of the AuNPs/MWNTs nanohybrids based sensor was detected. Sensing interfaces prepared on the same and on different electrodes were used to examine PKA activity with the same concentration. Standard deviation of three dependent measurements was less than 4.1% for the same electrode, and less than 8.8% for different electrodes. Thus, the electrochemical sensor has a relatively good reproduction in PKA activity detection.

3.6. *Influence of inhibitor on PKA activity*

To further validate the potential application of this electrochemical method in the inhibition assay, the experiment of the influence of inhibitor on PKA activity was performed. Herein, the ellagic acid, reported as a cell-permeable and potent antioxidant, was used as a model inhibitor [42]. As shown in Fig. 5B, the electrochemical signal decreased with increasing the concentration of ellagic acid, which revealed the inhibition of PKA and low levels of peptide phosphorylation. On the basis of the result, the IC_{50}, the half maximal inhibitory concentration, was estimated to be 3.98 μM. This result was in agreement with that reported in the literature obtained with a conventional kinase assay [31]. These results indicated that the AuNPs/MWNTs nanohybrids based on electrochemical assay have the potential ability to qualitatively screen the activity of the kinase inhibitor.

4. Conclusions

In conclusion, we have developed a simple and amplification electrochemical assay for PKA activity and inhibition analysis with the AuNPs/MWNTs nanohybrids. Here, the AuNPs/MWNTs nanohybrids exhibited the property of peroxidase-like activity and signal amplification. To the best of our knowledge, it was the first time that the electrochemical detection of kinase activity and inhibition was carried out by using the catalytic activity of AuNPs/MWNTs nanohybrids. Owing to the peroxidase-like activity and signals amplification of AuNPs/MWNTs nanohybrids, the electrochemical assay makes the electrochemical signal change in the presence of different enzymatic unit/ml of PKA. The results indicated that the AuNPs/MWNTs nanohybrids based electrochemical assay provided a sensitive assay for PKA kinase activity monitoring with a low detection limit of 0.09 U/mL. Furthermore, the method developed here shows potential applications in the accurate and quantitative kinase inhibitor assay. In addition, it was a general approach which can be ready for others kinase activities and inhibition assays.

Acknowledgments

This work was supported in part by the Key Project of Natural Science Foundation of China (Grant nos. 21175039, 21322509, 21305035, 21190044, and 21221003), the Research Fund for the Doctoral Program of Higher Education of China (Grant 20110161110016) and the project supported by the Hunan Provincial Natural Science Foundation and Hunan Provincial Science and Technology Plan of China (2012TT1003).

Appendix A. Supporting information

Supplementary data associated with this article can be found in the online version at http://dx.doi.org/10.1016/j.talanta.2014.05.043.

References

[1] S.S. Taylor, C. Kim, C.Y. Cheng, S.H.J. Brown, J. Wu, N. Kannan, Biochim. Biophys. Acta 1784 (2008) 16–26.
[2] P. Cohen, Nat. Rev. Drug Discov. 1 (2002) 309–315.
[3] J. Rush, A. Moritz, K.A. Lee, A. Guo, V.L. Goss, E.J. Spek, H. Zhang, X.M. Zha, R.D. Polakiewicz, M.J. Comb, Nat. Biotechnol. 23 (2005) 94–101.
[4] K.J. Way, N. Katai, G.L. King, Diabet. Med. 18 (2001) 945–959.
[5] K. Hensley, R.A. Floyd, N.Y. Zheng, R. Nael, K.A. Robinson, X. Nguyen, Q.N. Pye, C.A. Stewart, J. Geddes, W.R. Markesbery, E. Patel, G.V.W. Johnson, G. Bing, J. Neurochem. 72 (1999) 2053–2058.
[6] S.H. Park, K.C. Ko, M.H. Choi, J. Label. Compd. Radiopharm. 52 (2009) 422–426.
[7] X.H. Xu, X. Liu, Z. Nie, Y.L. Pan, M.L. Guo, S.Z. Yao, Anal. Chem. 83 (2011) 52–59.
[8] J. Bai, Y.J. Zhao, Z.B. Wang, C.H. Liu, Y.C. Wang, Z.P. Li, Anal. Chem. 85 (2013) 4813–4821.
[9] S. Shiosaki, T. Nobori, T. Mori, R. Toita, Y. Nakamura, C.W. Kim, T. Yamamoto, T. Niidome, Y. Katayama, Chem. Commun. 49 (2013) 5592–5594.
[10] R. Freeman, T. Finder, R. Gill, I. Willner, Nano Lett. 10 (2010) 2192–2196.
[11] G.C. Zhou, F. Khan, Q. Dai, J.E. Sylvester, S.J. Kron, Mol. BioSyst. 8 (2012) 2395–2404.
[12] T. Mori, K. Inamori, Y. Inoue, X.M. Han, G. Yamanouchi, T. Niidome, Y. Katayama, Anal. Biochem. 375 (2008) 223–231.
[13] X.H. Xu, J. Zhou, X. Liu, Z. Nie, M. Qing, M.L. Guo, S.Z. Yao, Anal. Chem. 84 (2012) 4746–4753.
[14] O. Wilner, C. Guidotti, A. Wieckowska, R. Gill, I. Willne, Chem.—Eur. J. 14 (2008) 7774–7781.
[15] N. Qu, B. Wan, L.H. Guo, Analyst 133 (2008) 1246–1249.
[16] C.L. Wang, L.Y. Wei, C.J. Yuan, K.C.H. Wang, Anal. Chem. 84 (2011) 971–977.
[17] Y. Yang, L.H. Guo, N. Qu, M.Y. Wei, L.X. Zhao, B. Wan, Biosens. Bioelectron. 28 (2011) 284–290.
[18] S. Martic, M. Labib, H.B. Kraatz, Talanta 85 (2011) 2430–2436.
[19] S. Martic, S. Tackenburg, Y. Bilokin, A. Golub, V. Bdzhola, S. Yarmoluk, H.B. Kraatz, Anal. Biochem. 421 (2012) 617–621.
[20] P. Miao, L.M. Ning, X.X. Li, P.F. Li, G.X. Li, Bioconj. Chem. 23 (2012) 141–145.
[21] K. Kerman, M. Chikae, S. Yamamura, E. Tamiya, Anal. Chim. Acta 588 (2007) 26–33.
[22] K. Kerman, H.B. Kraatz, Biosens. Bioelectron. 24 (2009) 1484–1489.
[23] Z.F. Chen, X.X. He, Y.H. Wang, K.M. Wang, Y.D. Du, G.P. Yan, Biosens. Bioelectron. 41 (2013) 519–525.
[24] J. Ji, H. Yang, Y. Liu, H. Chen, J.L. Kong, B.H. Liu, Chem. Commun. 12 (2009) 1508–1510.
[25] X.X. He, Z.F. Chen, Y.H. Wang, K.M. Wang, J. Su, G.P. Yan, Biosens. Bioelectron. 35 (2012) 134–139.
[26] K. Saha, S.S. Agasti, C. Kim, X.N. Li, V.M. Rotello, Chem. Rev. 112 (2012) 2739–2779.
[27] J. Zeng, Q. Zhang, J.Y. Chen, Y.N. Xia, Nano Lett. 10 (2010) 30–35.
[28] X.H. Xu, Z. Nie, J.H. Chen, Y.C. Fu, W. Li, Q.P. Shen, S.Z. Yao, Chem. Commun. 0 (2009) 6946–6948.
[29] Z. Zhao, X.M. Zhou, D. Xing, Biosens. Bioelectron. 31 (2012) 299–304.
[30] J. Wang, Y. Cao, Y. Li, Z.Q. Liang, G.X. Li, J. Electroanal. Chem. 656 (2011) 274–278.
[31] S.J. Xu, Y. Liu, T.H. Wang, J.H. Li, Anal. Chem. 82 (2010) 9566–9572.
[32] Z.Y. Zhang, A. Berg, H. Levanon, R.W. Fessenden, D. Meisel, J. Am. Chem. Soc. 125 (2003) 7959–7963.
[33] A. Corma, H. Garcia, Chem. Soc. Rev. 37 (2008) 2096–2126.
[34] Y. Jv, B.X. Li, R. Cao, Chem. Commun. 46 (2010) 8017–8019.
[35] Y.F. Zhang, C.L. Xu, B.X. Li, Y.B. Li, Biosens. Bioelectron. 43 (2013) 205–210.
[36] C. Gao, Z. Guo, J.H. Liu, X.J. Huang, Nanoscale 4 (2012) 1948–1963.
[37] J. Zhang, R.J. Lao, S.P. Song, Z.Y. Yan, C.H. Fan, Anal. Chem. 80 (2008) 9029–9033.
[38] G. Liu, Y. Wan, V. Gau, J. Zhang, L.H. Wang, S.P. Song, C.H. Fan, J. Am. Chem. Soc. 130 (2008) 6820–6825.
[39] T. Niidome, K. Nakashima, H. Takahashi, Y. Niidome, Chem. Commun. 17 (2004) 1978–1979.
[40] X. Yu, B. Munge, V. Patel, G. Jensen, A. Bhirde, J.D. Gong, S.N. Kim, J. Gillespie, J.S. Gutkind, F. Papadimitrakopoulos, J.F. Rusling, J. Am. Chem. Soc. 128 (2006) 11199–11205.
[41] Y. Tao, Y.H. Lin, Z.Z. Huang, J.S. Ren, X.G. Qu, Adv. Mater. 25 (2013) 2594–2599.
[42] G. Cozza, P. Bonvini, E. Zorzi, G. Poletto, M.A. Pagano, S. Sarno, A.D. Deana, G. Zagotto, A. Rosolen, L.A. Pinna, F. Meggio, S. Moro, J. Med. Chem. 49 (2006) 2363–2366.